Catalysis Today 156 (2010) 187–190

Contents lists available at ScienceDirect

Catalysis Today

journal homepage: www.elsevier.com/locate/cattod

Improved water dissociation and nitrous oxide decomposition by in situ oxygen removal in perovskite catalytic membrane reactor

Heqing Jiang[a,*], Haihui Wang[b], Fangyi Liang[a], Steffen Werth[a], Steffen Schirrmeister[c], Thomas Schiestel[d], Jürgen Caro[a,*]

[a] Institute of Physical Chemistry and Electrochemistry, Leibniz University of Hannover, Callinstr. 3A, D-30167 Hannover, Germany
[b] College of Chemistry and Chemical Engineering, South China University of Technology, Guangzhou, 510640, PR China
[c] Uhde GmbH, Friedrich-Uhde-Str. 15, D-44141 Dortmund, Germany
[d] Fraunhofer Institute of Interfacial Engineering and Biotechnology (IGB), Nobelstr 12, D-70569 Stuttgart, Germany

ARTICLE INFO

Article history:
Available online 21 March 2010

Keywords:
Membrane reactor
Water dissociation
Perovskite
N_2O decomposition
Oxygen removal

ABSTRACT

The equilibrium controlled water dissociation and the kinetically controlled nitrous oxide (N_2O) decomposition were studied in the perovskite $BaCo_xFe_yZr_{1-x-y}O_{3-\delta}$ (BCFZ) oxygen-permeable membrane reactor. By increasing the temperature or pressure difference and by feeding reducing gases like methane or ethane to the permeate side to consume the permeated oxygen, hydrogen production rate or N_2O conversion could be enhanced. A hydrogen production rate of 3.1 $cm^3\ min^{-1}\ cm^{-2}$ was obtained at 950 °C. When methane was used as the reducing gas on the shell side, the oxygen concentration on the N_2O side can be kept at a low level, thus avoiding the inhibition of the N_2O decomposition by adsorbed surface oxygen species. A complete decomposition of N_2O for gas streams containing 20 vol.% N_2O was achieved on the core side at 850 °C. Simultaneously, methane on the shell side was converted into synthesis gas with CO yield of above 80%. When feeding ethane to the shell side, the hydrogen from the thermal dehydrogenation of ethane can consume the permeated oxygen. At 850 °C, an ethane conversion of 85% and an ethylene selectivity of 86% were obtained.

1. Introduction

In the past two decades, membrane reactors, as devices combining chemical reactions and a membrane separation in one unit, have attracted more and more attention [1–3]. One of the major advantages of membrane reactors is that the equilibrium constraint of many reversible reactions can be overcome by removal of one or more product(s) through the membrane, thus further increasing the conversion. For example, the equilibrium constant of water dissociation is very small even at a relatively high temperature. However, significant amounts of H_2 from water splitting can be obtained at moderate temperatures if an oxygen-permeable membrane [4–7] is used to remove O_2 as it is generated [8–10]. In another application, a higher conversion can be obtained in membrane reactor if the reaction is kinetically limited and inhibited by one of the products. For example, for the catalytic decomposition of nitrous oxide (N_2O) [11–14] over perovskite catalysts, most of the catalysts cannot tolerate the co-existence of O_2 because adsorbed oxygen blocks the catalytically active sites for the N_2O decomposition [15,16]. However, the total decomposition of N_2O can be obtained in a perovskite catalytic membrane reactor if the inhibitor oxygen is continually removed from the N_2O side of the membrane [17].

Obviously, the performance of the membrane reactor used for water splitting or N_2O decomposition depends directly on the rate of oxygen removal from the system. In this work, a novel $BaCo_xFe_yZr_{1-x-y}O_{3-\delta}$ (BCFZ) hollow fiber perovskite membrane was employed to in situ remove O_2 from water dissociation or N_2O decomposition. This BCFZ hollow fiber membrane exhibits a high oxygen permeation rate and has already been used, for example, in the production of oxygen-enriched air [18] and the partial oxidation of hydrocarbons [19,20]. Special attention was given to the effect of oxygen permeability of the BCFZ membrane on the reactor performance for water splitting or N_2O decomposition.

2. Experimental

The dense BCFZ perovskite hollow fiber membranes were manufactured by a phase inversion process [21]. After sintering, the fiber has a thickness of around 0.17 mm with outer diameter of 1.10 mm and inner diameter of 0.76 mm. Fig. 1 shows a schematic diagram of the membrane reactor used in this study. Two ends of the hol-

* Corresponding author. Tel.: +49 511 7622942; fax: +49 511 76219121.
E-mail addresses: heqing.jiang@pci.uni-hannover.de, hq.jiang@yahoo.com (H. Jiang), juergen.caro@pci.uni-hannover.de (J. Caro).

0920-5861/$ – see front matter © 2010 Elsevier B.V. All rights reserved.
doi:10.1016/j.cattod.2010.02.027

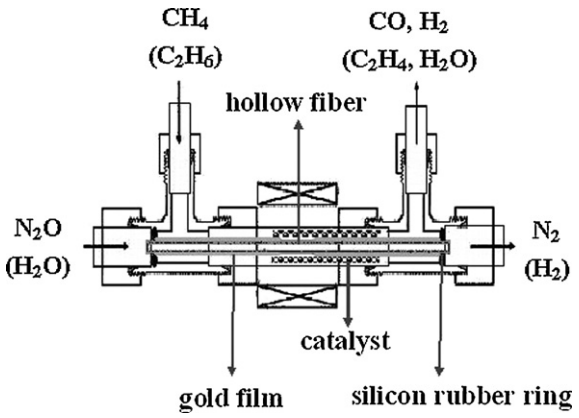

Fig. 1. Schematic diagram of membrane reactors for water splitting and N_2O decomposition.

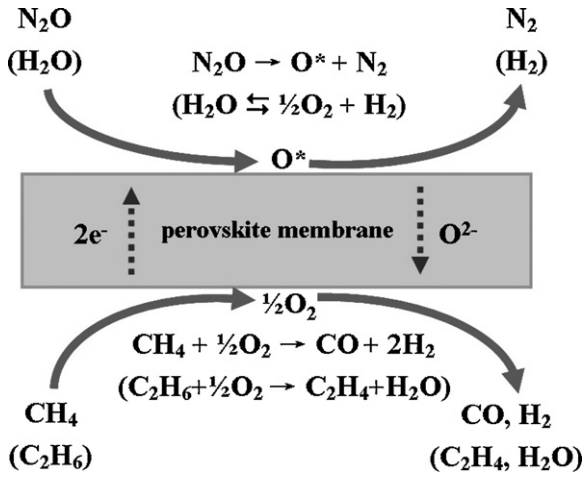

Fig. 2. Concept of water splitting and N_2O decomposition in a perovskite oxygen-permeable membrane reactor.

low fiber were coated by Au paste (C5754, Heraeus GmbH) and then sintered at 950 °C for 5 h. The coating and sintering procedure were repeated three times and a dense Au film which is not permeable to oxygen was obtained on BCFZ membrane surface. Such Au-coated hollow fiber can be sealed by silicon rubber ring and the uncoated part (the effective length is 3 cm, and the effective membrane area is 0.86 cm^2) which is permeable to the oxygen can be kept in the middle of the oven ensuring isothermal conditions. The mixture of N_2O (or H_2O) and He was fed to the core side and a mixture of CH_4 (or C_2H_6), Ne and He was fed to the shell side. A Ni-based steam reforming (SR) catalyst (Süd Chemie AG) was packed around and behind the hollow fiber membrane when methane was used as the reducing gas on the shell side. N_2O, CH_4, C_2H_6, He and Ne flow rates were controlled by gas mass flow controllers (Bronkhorst). H_2O flow rate was controlled by the liquid mass flow controller (Bronkhorst) and was completely evaporated at 180 °C before it was fed to the reactor. All gas lines to the reactor and the gas chromatograph were heated to 180 °C. The concentrations of the gases at the exit of the reactor were determined by an on-line gas chromatograph (Agilent 6890). Only very small amounts of oxygen (below 0.001%) and also nitrogen (below 0.007%) were detected, which probably come from the residual air in the metal lines. So, it was assumed that the oxygen from water splitting on the core side was totally removed and the flow rate at the outlet is equal to that at the inlet, and H_2 production rate on the core side was calculated from the total flow rate F_{core} ($cm^3\ min^{-1}$), the hydrogen concentration c (H_2), and the effective membrane area S (cm^2) based on the following equation:

$$J(H_2) = \frac{F_{\text{core}} \times c(H_2)}{S}$$

The N_2O conversion $X(N_2O)$, the C_2H_6 conversion $X(C_2H_6)$, and the C_2H_4 selectivity $S(C_2H_4)$ were calculated as

$$X(N_2O) = \left(1 - \frac{F(N_2O,\ \text{out})}{F(N_2O,\ \text{in})}\right) \times 100\%$$

$$X(C_2H_6) = \left(1 - \frac{F(C_2H_6,\ \text{out})}{F(C_2H_6,\ \text{in})}\right) \times 100\%$$

$$S(C_2H_4) = \frac{F(C_2H_4,\ \text{out})}{F(C_2H_6,\ \text{in}) - F(C_2H_6,\ \text{out})} \times 100\%$$

where $F(i)$ is the flow rate of species i on the shell or core side of the hollow fiber membrane.

3. Results and discussion

3.1. The concept of water splitting and N_2O decomposition in membrane reactor

Water dissociation into hydrogen and oxygen is a reversible reaction, and the equilibrium constant of this reaction is very small even at a relatively high temperature. According to the low equilibrium constant of $K_p \approx 2 \times 10^{-8}$ at 950 °C [22], only very low equilibrium concentrations of $P_{O2} \approx 4.6 \times 10^{-6}$ bar and $P_{H2} \approx 9.2 \times 10^{-6}$ bar can be obtained. However, when this reaction is performed in the perovskite oxygen-permeable membrane reactor, as shown in Fig. 2, oxygen can permeate to the other side of the membrane where it is consumed by the partial oxidation of methane (POM) to form synthesis gas. Thus, oxygen and hydrogen become separated and the equilibrium of the water dissociation is continuously shifted to the product side.

Different to the equilibrium controlled water dissociation, the decomposition of N_2O is kinetically limited and inhibited by the product molecule oxygen. As shown in Fig. 2, the inhibitor O* can be removed as oxygen ion (O^{2-}) via the membrane as it is generated from N_2O on perovskite membrane surface according to $N_2O \rightarrow N_2 + O^*$. The local charge neutrality can be maintained by the counter diffusion of electrons (e^-). To increase the driving force for the oxygen transport through the membrane, methane or ethane can be fed to the permeate side of the membrane to consume the permeated oxygen.

3.2. Hydrogen production from water splitting

It was experimentally found that, if only inert gas was used as sweep on the shell side, the H_2 production rate on the steam side is very low. As shown in H_2 chromatograms (the inset of Fig. 3), hydrogen is hardly detectable even at 900 °C. However, H_2 was observed when feeding methane in combination with a Ni-based catalyst to the shell side, which is more effective to consume the permeated O_2 and establish a larger O_2 partial pressure gradient across the membrane. Because H_2 production rate depends directly on the rate of O_2 removal from water dissociation, it can be increased by increasing the temperature or a steeper oxygen partial pressure gradient across the membrane according to Wagner theory [23,24]. It can be seen from Fig. 3 that the hydrogen production rate increases from 0.7 to 3.1 $cm^3\ min^{-1}\ cm^{-2}$ as the temperature rises from 800 to 950 °C. Moreover, it was also found that increasing the concen-

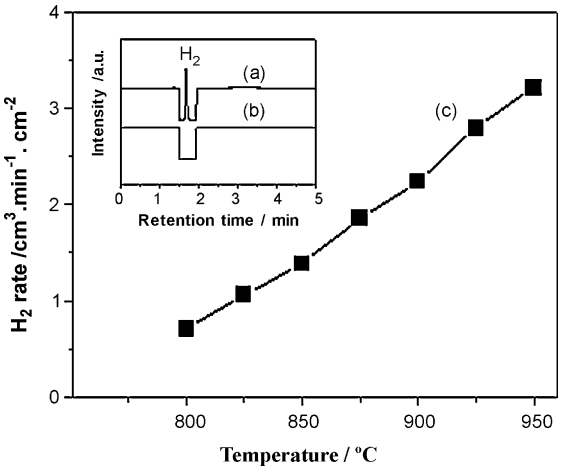

Fig. 3. H_2 production rate on the core side as a function of temperature. The inset shows H_2 chromatograms at 900 °C. Core side (a, b and c): F_{H2O} = 30 cm³ min⁻¹ and F_{He} = 10 cm³ min⁻¹. Shell side (a and c): 50 cm³ min⁻¹ (F_{He} = 45 cm³ min⁻¹, F_{Ne} = 3 cm³ min⁻¹ and F_{CH4} = 2 cm³ min⁻¹). Shell side (b): 50 cm³ min⁻¹ (F_{He} = 47 cm³ min⁻¹ and F_{Ne} = 3 cm³ min⁻¹). Amount of packed bed Ni/Al_2O_3 catalyst: 0.8 g.

tration of steam in the feed gas will shift the equilibrium towards the water dissociation and more H_2 can be produced.

3.3. Direct decomposition of N_2O coupled with partial oxidation of methane

Fig. 4 presents N_2O conversion and oxygen concentration at the exit of N_2O side at different temperatures without and with oxygen removal. It can be seen that the conversion of N_2O increases with increasing temperature. When there is no sweep gas flow on the shell side, however, the conversion is relatively low (below 30% even at 900 °C) since the produced oxygen from the N_2O decomposition was not removed and – as a result – the oxygen concentration at the exit of N_2O side increases when the temperature rises from 750 to 900 °C, as shown in Fig. 4a′. To obtain a higher conversion of N_2O decomposition, the adsorbed surface oxygen O* should be removed fast. As shown in Fig. 4b′, when diluted methane was fed to the shell side, the oxygen concentration at the exit of N_2O side decreases with increasing temperature because the oxygen from N_2O decomposition can be effectively removed in this case. Accordingly, the conversion of N_2O decomposition was significantly improved, as shown in Fig. 4b. When the temperature reaches 850 °C, N_2O in a concentration of 20 vol.% on the core side was totally decomposed.

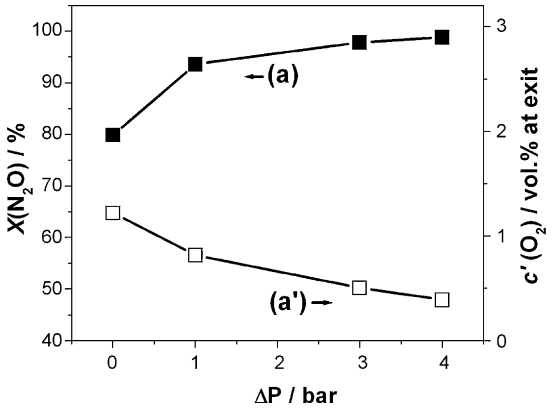

Fig. 5. N_2O conversion (a) and oxygen concentration (a′) at the exit of N_2O side as a function of pressure difference. Core side: F_{N2O} = 6 cm³ min⁻¹, F_{He} = 24 cm³ min⁻¹, P = 1.0–5.0 bar. Shell side: 40 cm³ min⁻¹ (F_{CH4} = 8 cm³ min⁻¹, F_{Ne} = 12 cm³ min⁻¹ and F_{H2O} = 20 cm³ min⁻¹), P = 1 bar, T = 800 °C. Amount of packed bed Ni/Al_2O_3 catalyst: 1.2 g.

As mentioned above, the conversion of N_2O decomposition is related to the oxygen permeability of the membrane. According to Wagner equation, the oxygen permeation rate can be improved by increasing the oxygen partial pressure gradient across the membrane. Fig. 5 shows the influence of pressure difference on the N_2O conversion and oxygen concentration at the exit of N_2O side at 800 °C. It can be seen that N_2O conversion increases with rising pressure difference because more oxygen from N_2O decomposition can be transported to the other side of the membrane in the case of a steeper oxygen partial pressure gradient. It was found that the N_2O conversion increased from 80% to 99% when changing the pressure difference from 0 to 4 bar. Accordingly, the oxygen concentration at exit of N_2O side decreased gradually with increasing pressure difference due to the depletion of N_2O, as shown in Fig. 5a′.

In order to investigate the effect of the presence of external oxygen in the feed gas on N_2O abatement in this membrane reactor, different amounts of oxygen were added to the N_2O/He co-feed on the core side. From Fig. 6, we can see that N_2O conversion decreased with increasing oxygen concentration in the N_2O/O_2 co-feed gas at 800 °C. Oxygen cannot become totally removed due to the limited oxygen permeability of this membrane at this temperature, which

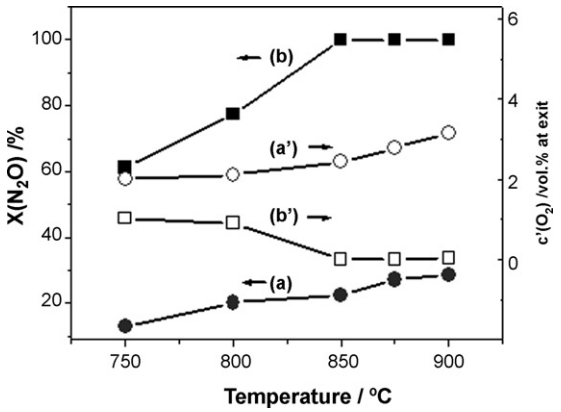

Fig. 4. N_2O conversion and oxygen concentration at exit of N_2O side as a function of temperature without (a and a′) or with (b and b′) oxygen removal. Core side: F_{N2O} = 6 cm³ min⁻¹, F_{He} = 24 cm³ min⁻¹. Shell side: (a and a′) no feed gas or (b and b′) 40 cm³ min⁻¹ (F_{CH4} = 8 cm³ min⁻¹, F_{Ne} = 12 cm³ min⁻¹ and F_{H2O} = 20 cm³ min⁻¹). Amount of packed bed Ni/Al_2O_3 catalyst: 1.2 g.

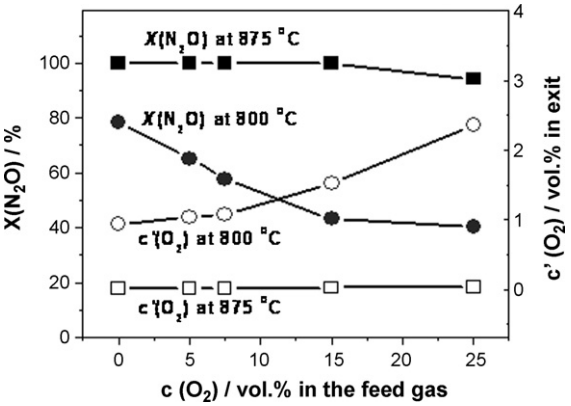

Fig. 6. N_2O conversion and oxygen concentration at the exit of N_2O side as a function of oxygen concentration in the N_2O/O_2 co-feed gas. Core side: 30 cm³ min⁻¹ (F_{N2O} = 6 cm³ min⁻¹, F_{O2} = 1.5–7.5 cm³ min⁻¹, F_{He} = balance). Shell side: 40 cm³ min⁻¹ (F_{CH4} = 18 cm³ min⁻¹, F_{H2O} = 22 cm³ min⁻¹). Amount of packed bed Ni/Al_2O_3 catalyst: 1.2 g.

Table 1
C_2H_6 conversion $X(C_2H_6)$, C_2H_4 selectivity $S(C_2H_4)$ and N_2O conversion $X(N_2O)$ at different temperatures.

Temperature/°C	$X(C_2H_6)$/%	$S(C_2H_4)$/%	$X(N_2O)$/%
800	57	88	68
850	85	86	100
875	91	80	100

Core side: F_{N2O} = 1.5 cm^3 min^{-1}, F_{He} = 28.5 cm^3 min^{-1}. Shell side: 50 cm^3 min^{-1} (F_{C2H6} = 11.5 cm^3 min^{-1}, F_{Ne} = 1 cm^3 min^{-1}, F_{He} = 32.5 cm^3 min^{-1} and F_{H2O} = 5 cm^3 min^{-1}).

can be further confirmed by the fact that the oxygen concentration at exit increased with increasing oxygen concentration in the co-feed gas. The excess oxygen will produce an inhibition effect on N_2O decomposition. However, N_2O conversion reached 99% and did not change with increasing oxygen concentration in the co-feed gas at 875 °C. According to the high oxygen permeability of BCFZ membrane at this temperature, all the oxygen can be removed from the N_2O side as shown in Fig. 6. These results show that the active surface of BCFZ membrane employed for N_2O abatement was not poisoned by adsorbed oxygen at high temperatures.

The permeated oxygen from N_2O decomposition can be used to produce synthesis gas by the POM on the shell side. According to a previous study [19], the so-called POM process using a Ni-based catalyst is first a total oxidation of methane to H_2O and CO_2, which is followed by steam and CO_2 reforming. A methane conversion of over 90% and CO selectivity of 90% were obtained at 875 °C. When oxygen is provided by thermal splitting of water, only limited amounts of oxygen were transported to methane side due to the very low equilibrium constant of water dissociation, and it was found that only 2 cm^3 min^{-1} methane can be converted into synthesis gas with methane conversion of 70% and CO selectivity of 60% [10]. Here, it was found that around 20 cm^3 min^{-1} methane can be converted into synthesis gas with CO yield of above 80% when N_2O was used to provide oxygen, indicating that N_2O decomposes easier than water to provide oxygen in the membrane reactor.

3.4. Direct decomposition of N_2O coupled with dehydrogenation of ethane

From the above discussion, to achieve the total decomposition of N_2O, a reducing gas should be used on the permeate side to consume the permeated oxygen, thus ensuring a large driving force for the fast oxygen removal from N_2O side. Besides methane, ethane was also used as the reducing gas in this paper. At high temperature, the thermal dehydrogenation of ethane leads to the formation of ethylene and hydrogen according to Eq. (1).

$$C_2H_6 \leftrightarrows C_2H_4 + H_2 \quad (1)$$

The produced hydrogen can be used to consume the permeated oxygen from N_2O side based on Eq. (2).

$$H_2 + 1/2O_2 \rightarrow H_2O \quad (2)$$

From Table 1, it can be found that, on increasing the temperature from 800 to 875 °C, ethane conversion increases from about 57% to 91%. Besides C_2H_4, H_2, H_2O and C_2H_6, CO and CO_2 were also detected in the effluents. Simultaneously, with rising temperature, N_2O conversion increased from 68% to almost 100% due to the increasing oxygen permeation rate. The ethylene selectivity decreases from 88% to 80%, the concentrations of CO increase from 1% to 4%, and the concentrations of CO_2 increase from 0.4% to 0.7%. An increasing amount of methane was also found in the product stream from the shell side of BCFZ membrane. In the dehydrogenation of C_2H_6 to C_2H_4, in addition to the combustion of hydrogen by the permeated oxygen, the deep oxidation of C_2H_4 to CO and CO_2 could not be avoided in the hollow fiber membrane reactor.

4. Conclusions

By using a perovskite-type BCFZ oxygen-permeable hollow fiber membrane, oxygen from water dissociation can be continually removed, and the equilibrium of this reaction is continuously shifted to the product side. When feeding methane to the permeate side, a larger driving force was provided for oxygen transport through the membrane, and accordingly significant amounts of hydrogen can be produced. A hydrogen production rate of 3.1 cm^3 min^{-1} cm^{-2} was obtained at 950 °C. For the decomposition of N_2O over perovskite BCFZ, the surface adsorbed oxygen acts as an inhibitor. To obtain a higher N_2O conversion, the oxygen concentration on N_2O side should be kept at a very low level, which can be achieved by in situ removing the inhibitor oxygen via BCFZ hollow fiber membrane. It was found that the oxygen concentration on N_2O side can be kept at a low level by increasing the temperature or the pressure difference and by feeding reducing gases like methane or ethane on permeate side. Benefiting from the effective oxygen removal via the oxygen-permeable membrane, a complete decomposition of N_2O with the concentration of 20 vol.% was obtained at 850 °C. Moreover, the permeated oxygen was used to produce synthesis gas by the POM or ethylene by the dehydrogenation of ethane on the shell side. An ethane conversion of 85% and an ethylene selectivity of 86% were obtained at 850 °C.

Acknowledgements

The authors gratefully acknowledge the financial support of the BMBF for the project CaMeRa (Catalytic Membrane Reactor) and SynMem FKZ 03 X 2013D under the auspices of ConNeCat (Competence Network Catalysis).

References

[1] R. Dittmeyer, J. Caro, in: G. Ertl, H. Knözinger, F. Schüth, J. Weitkamp (Eds.), Handbook of Heterogeneous Catalysis, vol. 4, Wiley-VCH, Weinheim, 2008, p. 2221.
[2] J. Sunarso, S. Baumann, J.M. Serra, W.A. Meulenberg, S. Liu, Y.S. Lin, J.D. Costa, J. Membr. Sci. 320 (2008) 13.
[3] K. Sirkar, P. Shanbhag, A. Kovvali, Ind. Eng. Chem. Res. 38 (1999) 3715.
[4] Y.T. Liu, X.Y. Tan, K. Li, Catal. Rev.-Sci. Eng. 48 (2006) 145.
[5] C. Chen, S.J. Feng, S. Ran, D.C. Zhu, W. Liu, H.J.M. Bouwmeester, Angew. Chem. Int. Ed. 115 (2003) 5354.
[6] W.S. Yang, H.H. Wang, X.F. Zhu, L.W. Lin, Top. Catal. 35 (2005) 155.
[7] F.T. Akin, Y.S. Lin, AIChE. J. 48 (2002) 2298.
[8] U. Balachandran, T.H. Lee, S. Wang, S.E. Dorris, Int. J. Hydrogen Energy 29 (2004) 291.
[9] U. Balachandran, T.H. Lee, S.E. Dorris, Int. J. Hydrogen Energy 32 (2007) 4451.
[10] H.Q. Jiang, H.H. Wang, S. Werth, T. Schiestel, J. Caro, Angew. Chem. Int. Ed. 47 (2008) 9341.
[11] J. Pérez-Ramírez, F. Kapteijn, G. Mul, J.A. Moulijn, Chem. Commun. 11 (2001) 693.
[12] G. Centi, A. Galli, B. Montanari, S. Perathoner, A. Vaccari, Catal. Today 35 (1997) 113.
[13] N. Russo, D. Fina, G. Saracco, V. Specchia, Catal. Today 119 (2007) 228.
[14] E.V. Kondratenko, O. Ovsitser, Angew. Chem. Int. Ed. 47 (2008) 2983.
[15] N. Gunasekaran, S. Rajadurai, J.J. Carberry, Catal. Lett. 35 (1995) 373.
[16] N. Russo, D. Mescia, D. Fino, G. Saracco, V. Specchia, Ind. Eng. Chem. Res. 46 (2007) 4226.
[17] H.Q. Jiang, H.H. Wang, F.Y. Liang, S. Werth, T. Schiestel, J. Caro, Angew. Chem. Int. Ed. 48 (2009) 2983.
[18] H.H. Wang, S. Werth, T. Schiestel, J. Caro, Angew. Chem. Int. Ed. 44 (2005) 6906.
[19] H.H. Wang, C. Tablet, T. Schiestel, S. Werth, J. Caro, Catal. Commun. 7 (2006) 907.
[20] H.H. Wang, C. Tablet, T. Schiestel, J. Caro, Catal. Today 118 (2006) 98.
[21] T. Schiestel, M. Kilgus, S. Peter, K.J. Caspary, H.H. Wang, J. Caro, J. Membr. Sci. 258 (2005) 1.
[22] S. Ihara, Bull. Electrotech. Lab. 41 (1977) 259.
[23] M. Schroeder, Phys. Chem. Chem. Phys. 7 (2005) 166.
[24] R. Merkle, J. Maier, H.J.M. Bouwmeester, Angew. Chem. Int. Ed. 43 (2004) 5069.